Journal Article

Investigation into ultrathin CdTe solar cell Voc using SCAPS modelling

Clayton, A.J., Di Carlo, V., Irvine, S.J.C., Barrioz, V. and Lamb, D.A.

Recommended citation:
Clayton, A.J., Di Carlo, V., Irvine, S.J.C., Barrioz, V. and Lamb, D.A. (2014), 'Investigation into ultrathin CdTe solar cell Voc using SCAPS modelling', *Materials Research Innovations*, Vol. 18, No.7, pp.505-508. doi: 10.1179/1433075X14Y.0000000259

Investigation into ultra-thin CdTe solar cell V_{oc} using SCAPS modelling

Andrew J. Clayton*, Virginia Di Carlo, Stuart J. C. Irvine, Giray Kartopu, Vincent Barrioz and Dan A. Lamb

Centre for Solar Energy Research (CSER), Glyndŵr University, OpTIC, Ffordd William Morgan, St. Asaph Business Park, Denbighshire, LL17 0JD, UK
Email: a.clayton@glyndwr.ac.uk; Tel: 44 1745 535 213

Abstract

Ultra-thin CdTe photovoltaic solar cells were produced by metal organic chemical vapour deposition in a single horizontally configured growth chamber. Solar cell activation was investigated by varying the duration of the $CdCl_2$ layer deposition and 420 °C thermal anneal to promote Cl diffusion into the CdTe. Thicker $CdCl_2$ layers used in activation treatment resulted in a greater degree of sulphur interdiffusion, up to 2 at.%, into the CdTe layer. The thicker $CdCl_2$ activation layer was necessary to lower the reverse saturation current density for obtaining optimum experimental photovoltaic (PV) device performances. Modelling of the PV performances with equivalent solar cell structure for optimised devices using Solar Cell Capacitance Simulation software resulted in an overestimated open circuit voltage (V_{oc}). The simulations showed that reduced acceptor states at the CdTe interface with the intermixed region resulted in the largest decrease in V_{oc} when considering large back surface recombination velocities.

Keywords: MOCVD; ultra-thin CdTe; Photovoltaics; Modelling

1. Introduction

CdTe has the largest share of the thin film photovoltaic (PV) market [1] and with recent improvements to the world record cell efficiency, which is currently at 20.4% [2] should continue to receive commercial interest for solar module production. However, due to uncertainty of future global tellurium stock reserves [3, 4] consideration towards reduced material consumption, as well as improved materials utilization and recycling of waste material and/or end-of-life modules is necessary for continued large-scale industrial production of thin film CdTe [1].

Thicknesses from 2 to 8 μm are typically used for the CdTe absorber even though the majority of photons are absorbed in the first one μm [3]. Reducing materials consumption has been the focus of this paper, where using thinner coatings has the added benefit of lowering manufacturing costs, provided reasonable device efficiencies are still achievable.

This paper reports on the materials challenges associated with ultra-thin $Cd_{1-x}Zn_xS$/CdTe PV solar cells where both short circuit current density (J_{sc}) and the open circuit voltage (V_{oc}) decrease with absorber layer thickness. The effect of $CdCl_2$ activation treatment on the dark saturation current density (J_0) and ideality factor (n)

has been investigated for ultra-thin CdTe cells and related to PV performances. Comparison has also been made to solar cell capacitance simulation (SCAPS) [5] addressing the sulphur interdiffusion effect, which forms a $CdTe_{1-y}S_y$ phase at the metallurgical interface [6] with a sulphur tail extending to the back contact region in the ultra-thin cells [7].

2. Experimental methods

Ultra-thin $Cd_{1-x}Zn_xS$/CdTe solar cells were produced using metal organic chemical vapour deposition (MOCVD) in a single growth chamber. Commercial boro-aluminosilicate glass coated with indium tin oxide (ITO) was used as the substrate, with thickness of 1.1 mm and sheet resistance of 4-10 Ω/□. As was used as the CdTe acceptor dopant with concentration in the range [As] ~10^{18} - 10^{19} atoms/cm^3. Further deposition parameters have been detailed previously [8]. The solar cell spectral response in the blue region of the solar spectrum was enhanced by using a wide band gap $Cd_{1-x}Zn_xS$ window layer, 0.24 µm in thickness [8-10]. Variable deposition and anneal times were used for an *in situ* $CdCl_2$ treatment process [11]. A CdTe absorber thickness of 0.5 µm was employed for all solar cells due to high sensitivity of the spectral response to the $CdCl_2$ activation treatments. Each CdTe solar cell device consisted of eight cells of area 0.25 cm^2, defined by evaporating gold (Au) through a mask. Solar cell characterisation has been detailed elsewhere [8].

Parameters used for the ultra-thin cells in the Solar Cell Capacitance Simulation (SCAPS) modelling were based on those used for devices with baseline (2.25 µm) CdTe thicknesses. Short circuit current density – voltage (*J-V*) measurements for experimental and simulated solar cells were in good agreement. The parameters for the baseline device were transferred to the simulation for the ultra-thin devices as a starting point. The effect on interface states in the simulation was investigated by systematically changing the acceptor defect concentration between 5 × 10^{13} and 5 × 10^{16} cm^{-2} at the $Cd_{1-x}Zn_xS$/interfacial layer interface, with a constant defect concentration of 1 × 10^{14} cm^{-2} at the interfacial layer/CdTe interface. The process was then repeated for the interfacial layer/CdTe interface whilst keeping the $Cd_{1-x}Zn_xS$/interfacial layer defect concentration constant at 5 × 10^{14} cm^{-2}. Back surface recombination was simulated by changing the recombination velocity between 1 × 10^4 and 1 × 10^8 cm/s at the back contact.

3. Results and discussion

The $CdCl_2$ deposition time for CdTe solar cell activation treatment was reduced by at least half for ultra-thin (CdTe = 0.5 µm) devices compared to the $CdCl_2$ deposition time used for baseline (CdTe = 2.25 µm) devices produced by the MOCVD process.

Generally, a surplus of $CdCl_2$ is used in order to achieve optimum defect passivation, with remaining $CdCl_2$ at the back surface being rinsed away with deionised water. For ultra-thin devices, the $CdCl_2$ annealing treatment was found [8, 12] to leach Zn out of the $Cd_{1-x}Zn_xS$ alloy window resulting in deterioration of photocurrent generation in the blue region of the solar spectrum due to the window alloy band gap (E_g) narrowing closer towards the CdS E_g. For this reason, the $CdCl_2$ deposition time was intentionally reduced to minimise Zn leaching within the ultra-thin CdTe solar cells. $CdCl_2$ deposition times of 179, 120, 80 and 0 s (reference device) were used for the ultra-thin CdTe solar cells relative to 359 s for the baseline (CdTe = 2.25 µm) device [7].

3.1 Reverse saturation current and ideality factor

Dark *J-V* curves were measured to calculate J_0 and n for the ultra-thin CdTe solar cells after variable $CdCl_2$ activation treatment. The relationship of J_0 and n to V_{oc} is given by

$$V_{oc} = \frac{nkT}{q} ln\left(\frac{J_l}{J_0} + 1\right) \quad (1)$$

where kT/q represents the thermal voltage. J_l is the light generated current density, which generally can be assumed to be the J_{sc}. Values of n typically range between one and two, where n = 1 represents an ideal diode with radiative recombination in the bulk absorber material. Minority carrier recombination in CdTe can occur due to interface states at the junction and when the surface recombination velocity at the back contact interface is high [13]. The back surface has been suggested [14] to have greater influence over carrier recombination for ultra-thin CdTe solar cells leading to a reduction in V_{oc}. Figure 1 shows n as a function of $CdCl_2$ deposition time for ultra-thin CdTe solar cells, with comparison to baseline CdTe devices.

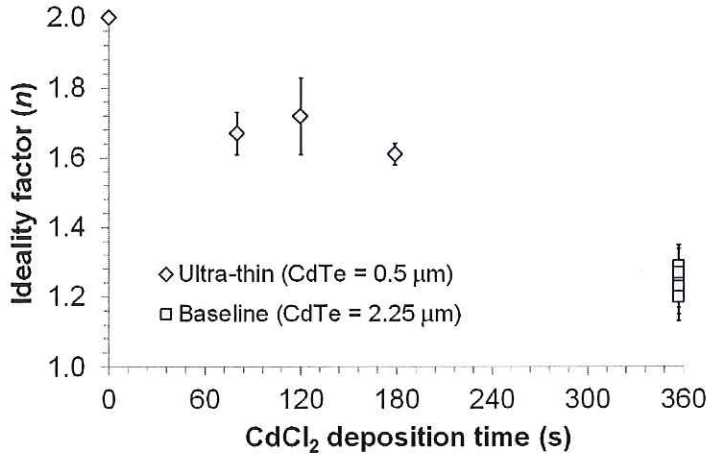

Figure 1: Ideality factor (n) calculated for ultra-thin CdTe solar cells deposited with different $CdCl_2$ deposition times (s) with comparison to a number of baseline CdTe solar cells.

Increased $CdCl_2$ activation treatment resulted in a fall in *n* due to greater defect passivation and reduction of mid-gap states that lead to carrier recombination [15]. The baseline thickness CdTe device *n* values were much lower than that for ultra-thin CdTe devices. This is because the depletion region and CdTe/back contact interface, being further apart, should have less influence on carrier recombination in baseline absorber thicknesses. J_0 also decreased with greater $CdCl_2$ activation treatment (Figure 2), which shows that if extrapolated to the $CdCl_2$ deposition times employed for the baseline devices, would still lead to values around two orders of magnitude above baseline J_0 values.

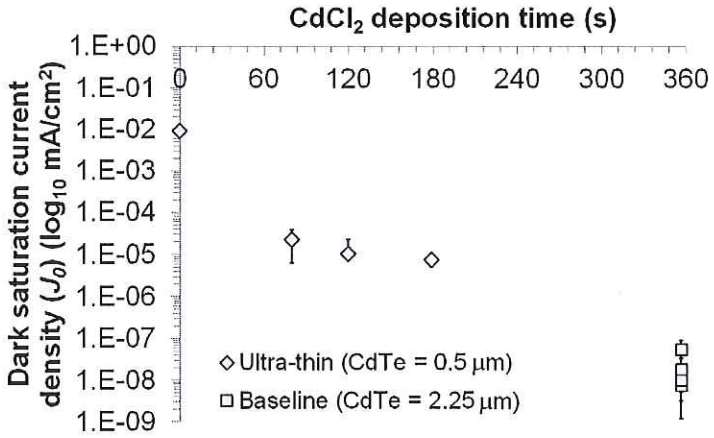

Figure 2: Saturation current density (J_0) calculated for ultra-thin and baseline CdTe solar cells with different $CdCl_2$ activation treatments.

3.2 P-type doping

V_{oc} can also be related to the acceptor concentration (N_A) using Equation (2) below:

$$V_{oc} = \frac{kT}{q} ln\left[\frac{(N_A+\Delta n)\Delta n}{n_i^2}\right] \quad (2)$$

where Δn and n_i are the excess and intrinsic carrier concentration, respectively. Increasing the p-type conductivity in CdTe is challenging due to its self-compensating nature which leads to the formation of donor states. For baseline devices produced by MOCVD it has been reported [10] that increased p-type doping with As towards the back contact is possible resulting in enhanced PV cell performance. Increased p-type doping was carried out for the ultra-thin CdTe solar cells throughout the absorber resulting in enhanced V_{oc} and overall improvement to PV performance relative to an equivalent solar cell device with lower p-type doping with As, as previously reported by Jones *et al.* [16]. The increased [As] in CdTe was used for the optimised ultra-thin device.

3.3 Sulphur interdiffusion

The degree of sulphur interdiffusion resulting in the formation of a $CdTe_{1-y}S_y$ phase increased with greater $CdCl_2$ activation treatment, correlating with enhancement of V_{oc} [12]. X-ray photoelectron spectroscopy (XPS) has revealed [7] that for ultra-thin CdTe solar cells the sulphur diffused from the window layer through the absorber and even reaching the back contact region. This may not be surprising, as sulphur is a fast diffuser and the CdTe absorber thickness is considerably reduced for ultra-thin solar cells. There was [12] a close correlation between both $CdCl_2$ deposition time and S content in CdTe versus V_{oc}, with a sulphur fraction equal to 2 at.% giving the highest V_{oc}.

3.4 SCAPS modelling

The MOCVD process employs Cd-rich conditions to promote As incorporation into the CdTe for extrinsic p-type doping. Parameters for donor defects based on interstitial Cd or Cd occupying a Te site within the CdTe layer were obtained from published sources [17, 18]. The SCAPS default acceptor defect parameter was used for the $Cd_{1-x}Zn_xS$ layer in the simulation. Acceptor defects at the interfaces with the intermixed layer in the junction region were defined from Proskuryakov *et al.* [17], with defect concentration of 5×10^{14} cm^{-2} at the interface with $Cd_{1-x}Zn_xS$ and 1×10^{14} cm^{-2} at the interface with CdTe. The back surface recombination velocity was kept at the default value of 1×10^8 cm/s. Increasing this value further did not lead to any changes in the simulation and this value was considered as a fast recombination velocity. Figure 3 shows the *J-V* curves for a baseline CdTe device with comparison to that generated from SCAPS, showing good agreement between the two curves.

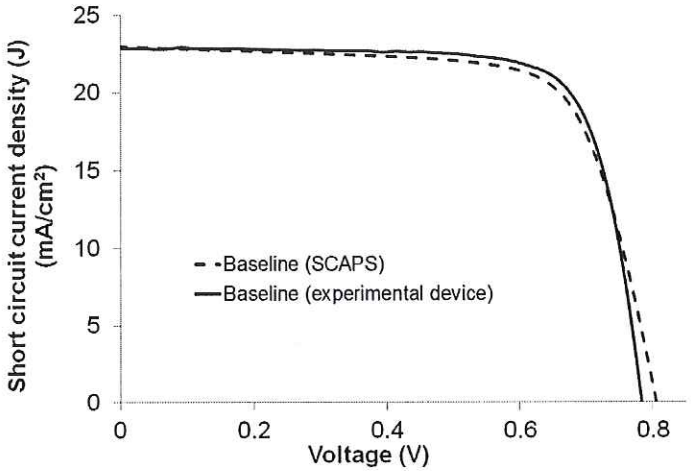

Figure 3: J-V curves for an experimental baseline (CdTe = 2.25 μm) device with comparison to a simulated curve for an equivalent device generated from SCAPS.

The defect parameters assigned to the baseline device were transferred to the ultra-thin simulations. For the ultra-thin device simulations, the level of sulphur diffusing into the CdTe was assumed to be at a uniform concentration of 2 at.% [12] to reflect the best performing PV device obtained experimentally. The $CdTe_{1-y}S_y$ phase E_g was manually set for the sulphur fraction at 2.0 at.% which was obtained from the calculation below:

$$E(y) = E_{CdTe} + (E_{CdS} - E_{CdTe} - b)y + by^2 \quad (3)$$

where E_{CdTe} is 1.45 eV, E_{CdS} is 2.42 eV, b is the bowing parameter at 2.0 eV and y is the sulphur fraction in the $CdTe_{1-y}S_y$ phase. The $CdTe_{1-y}S_y$ phase reduces in E_g for low levels of sulphur due to b being relatively large. This was accounted for in the simulation. The main differences in parameters between the baseline and ultra-thin devices used to define the solar cell structure are shown in Table 1.

Solar cell device	Baseline	Ultra-thin
CdTe thickness (µm)	2.25	0.5
CdTe layer structure	bilayer	single
As dopant conc. ($atoms/cm^3$)	1×10^{18}	1×10^{19}
	1×10^{19}	
$CdTe_{1-y}S_y$ phase (y = at.%)	0	2

Table 1: Baseline and ultra-thin CdTe solar cell structure differences.

The simulations were carried out with variations to the interface defects states as described in the Experimental section. Figure 4 shows the results of the simulated *J-V* curves with comparison to the best performing experimental ultra-thin solar cell.

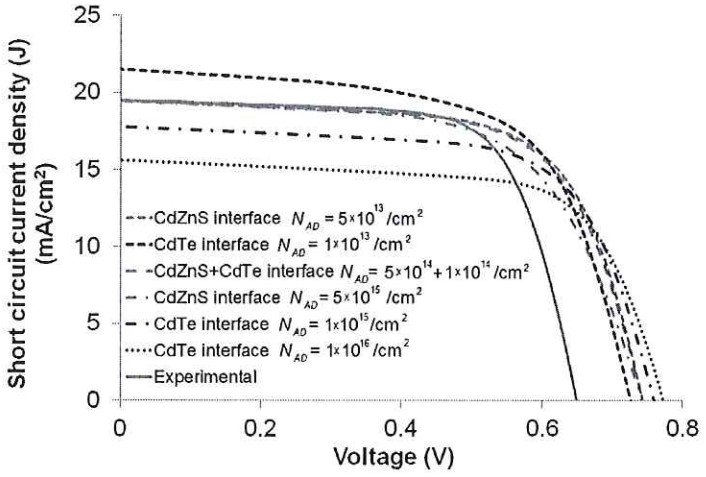

Figure 4: J-V curve comparison of an experimental ultra-thin CdTe PV device to simulated devices with varying concentration of interface defect states in the junction region.

Some variation to the V_{oc} was observed, but the change in the J_{sc} was more obvious, with values falling as low as 15 mA/cm^2 for higher acceptor sates at the CdTe interface. None of the simulations resulted in a V_{oc} that reflected the experimental device. It should be noted that the simulations were very simple and more complex changes could be occurring at the interface.

The back surface recombination velocity was then considered in the simulation. The defects at the interface were set back to that used for the baseline device as mentioned earlier in this section. Figure 5 shows the simulated *J-V* curves for ultra-thin devices considering different values for recombination velocity at the back surface. For low recombination velocity at the back surface both J_{sc} and V_{oc} are high. As the recombination velocity becomes more significant J_{sc} and V_{oc} fall. No further drop in these *J-V* parameters was observed for recombination velocities equal to 1 × 10^6 cm/s and higher.

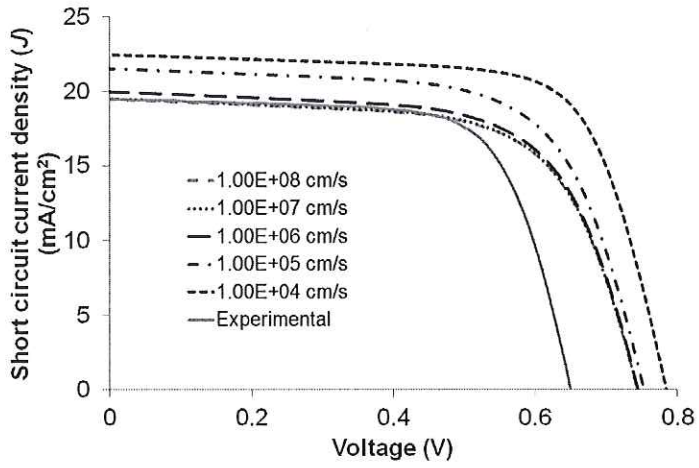

Figure 5: J-V curve comparison of an experimental ultra-thin CdTe PV device to simulated devices with varied recombination velocities at the back contact.

The SCAPS model used to simulate the *J-V* curves was configured with basic parameters. There may be a number of influences working together in the experimental device leading to the drop in V_{oc}, which have not been accounted for in the model. This may be due to an overlap of electric fields caused by the close proximity of the junction to the back contact resulting in amplified recombination rates at the back surface further deteriorating the V_{oc}.

4. Conclusions

Use of an ultra-thin absorber for CdTe solar cells results in a significant loss in V_{oc} compared to baseline devices due to a large increase in the reverse saturation current. Increased $CdCl_2$ activation treatment improved the V_{oc} by reducing the

saturation current, but it was evident by chart extrapolation that J_0 would remain higher than that for baseline devices after equivalent $CdCl_2$ activation treatment. Increased p-type doping in CdTe device using a higher concentration of As during deposition improved ultra-thin solar cell performances by boosting the V_{oc} to a certain degree. SCAPS was used to model the ultra-thin CdTe solar cells as a function of defect concentration at the interfaces in the junction region and as a function of recombination velocity at the back contact. V_{oc} was significantly larger for simulated ultra-thin CdTe solar cells relative to that obtained experimentally. It is likely that carrier recombination is increased in the junction region as well as at the back contact. This may be a result of an overlap in electric fields due to the close proximity of the junction region to the back contact region leading to higher recombination rates than could be accounted for in the simulation.

Acknowledgements

The authors would like to thank the EPSRC / TSB / Welsh Government funded SPECIFIC project for financial support and technical assistance. The authors are also grateful for the free access to the SCAPS software from Marc Burgelman and his team at Gent University, Belgium.

References

1. M. Marwede and A. Reller, *Resources, Conservation and Recycling* 69 (2012) 35.
2. M.A. Green, K. Emery, Y. Hishikawa, W. Warta, E.D. Dunlop, Solar cell efficiency tables (version 44), *Progress in Photovoltaics: Research and Applications* 22 (2014) 701.
3. A. Gupta, V. Parikh and A.D. Compaan, *Solar Energy Materials & Solar Cells* 90 (2006) 2263.
4. C. Candelise, J.F. Speirs and R.J.K. Gross, *Renewable and Sustainable Energy Reviews* 15 (2012) 4972.
5. M. Burgelman, J. Verschraegen, S. Degrave, P. Nollet, *Thin Solid Films* 480–481 (2005) 392.
6. P.N. Gibson, M.A. Baker and M.E. Özsan, *Surface and Interface Analysis* 33 (2002) 825.
7. A.J. Clayton, M.A. Baker, S. Babar, P.N. Gibson, S.J.C. Irvine, G. Kartopu, D.A. Lamb and V. Barrioz, *submitted for publication*.
8. A.J. Clayton, S.J.C. Irvine, E.W. Jones, G. Kartopu, V. Barrioz and W.S.M. Brooks, *Solar Energy Materials & Solar Cells* 101 (2012) 68.
9. G. Kartopu, A.J. Clayton, W.S.M. Brooks, S.D. Hodgson, V. Barrioz, A. Maertens, D.A. Lamb and S.J.C. Irvine, *Progress in Photovoltaics: Research and Applications* 22 (2014) 18.

10. S.J.C. Irvine, V. Barrioz, D. Lamb, E.W. Jones and R.L. Rowlands-Jones, *Journal of Crystal Growth* 310 (2008) 5198.
11. V. Barrioz, S.J.C. Irvine. E.W. Jones, R.L. Rowlands and D.A. Lamb, *Thin Solid Films* 515 (2007) 5808.
12. A.J. Clayton, S. Babar, M.A. Baker, G. Kartopu, D.A, Lamb, V. Barrioz and S.J.C. Irvine, *Proceedings of the 28th EUPVSEC*, Paris, 2013, 3AO6.5.
13. D. Kuciauskas, A. Kanevce, J.M. Burst, J.N. Deunow, R. Dhere, D.S. Albin, D.H. Levi and R.K. Ahrenkiel, Journal of Photovoltaics 4 (2013) 1319.
14. V. Plotnikov, X. Liu, N. Paudel, D. Kwon, K.A. Wieland, A.D. Compaan, *Thin Solid Films* 519 (2011) 7134.
15. J. Versluys, P. Clauws, P. Nollet, S. Degrave and M. Burgelman, *Thin Solid Films* 451-452 (2004) 434.
16. E.W. Jones, V. Barrioz, S.J.C. Irvine and D. Lamb, *Thin Solid Films* 517 (2009) 2226.
17. Y.Y.Proskuryakov, K.Durose, J.D.Major, M.K. Al Turkestani, V. Barrioz, S.J.C. Irvine, E.W. Jones, *Solar Energy Materials and Solar Cells* 93 (2009) 1572.
18. S.H. Wei, S.B. Zhang, *Physical Review B* 66 (2002) 155211.